ISSN : 0974 - 7540 Volume 6 Issue 2

Research & Reviews On Electrochemistry

Full Paper

RREC, 6(2), 2015 [049-057]

Diffusion characteristics of the $LiFePO_4$/C composite in an electrolyte based on LiBOB

V.A.Galaguz*, O.V.Potapenko, E.V.Panov

Institute of General and Inorganic Chemistry of the Ukrainian National Academy of Sciences, Akademika Palladina Ave, 32/34, Kyiv 03142, (UKRAINE)

E-mail: vgalaguz@ukr.net

ABSTRACT

The behavior of a composite cathode material LiFePO4/C has been analyzed using the methods of chronopotentiometry, cyclic voltammetry (CV) and electrochemical impedance spectroscopy (EIS). The specific capacity of the $LiFePO_4$, synthesized by the solid state method, changes from 110 to 40 mA·h/g with an increasing of the current density from 0.1 to 10C. The values of the diffusion coefficient for the lithium ions (D_{Li}) using the CV method are $2.06 \cdot 10^{-14}$ and $1.07 \cdot 10^{-14}$ cm^2/s for the anodic and cathodic processes, respectively. The diffusion coefficients, calculated by the impedance spectroscopy data,have been change in the range of $4 \cdot 10^{-12}$ to $6 \cdot 10^{-16}$ cm^2/s and are in a good agreement with the cyclic voltammetry data.

KEYWORDS

$LiFePO_4$/C;
Cathode;
D_{Li};
Kinetics.

INTRODUCTION

Lithiated iron phosphate $LiFePO_4$ is a promising component for lithium ion batteries[1-3]. $LiFePO_4$was proposed as a cathode material for LIA in 1996[4-5]. Its advantages include low cost, compatibility with most of the anode materials, high specific capacitance ($Q_{teor.}$ = 170 mA·h/g) and a degree of stability to withstand a significant amount of charge/discharge cycles without significant changes in the specific characteristics. As most electrochemical parameters depends on the speed of charge/discharge of the electrode, particularly important is the problem of a reliable measurement of the diffusion rate of lithium ions in the electrode matrix material.

Information on the diffusion processes in intercalation materials is often prepared using the methods of potentiostatic step titration, *PST*[6-7], galvanostatic step titration, *GTS*[8-9], the electrode impedance spectroscopy, *EIS*[10-11] and cyclic voltammetry, *CV*[12-13] at low speeds of the potential sweep. It should be noted that lithium diffusion coefficient values even for the same nature electrodes may significantly differ depending on the method of synthesis, the particle size and morphology, as well as on the electrochemical methods.

The range of substantial differences in the values of specific capacitance and the diffusion coefficient of lithium samples LiFePO4, synthesized in various ways, is well illustrated by the data in

Full Paper

TABLE 1 : Comparison of physico-chemical and electrochemical characteristics of the $LiFePO_4$/C, synthesized by various methods

No.	Synthesis method for the $LiFePO_4$	Particle size	Specific surface area (S) $m^2 \cdot g^{-1}$ and actual electrode surface area (A) cm^2	Specific capacitance, Q, mA·h/g	Diffusion coefficient, cm^2/s	Reference
1	Solid state synthesis	8 μm	S = 32.7 $m^2 \cdot g^{-1}$ (BET) A = 14.38 cm^2	–	7.7×10^{-17} (EIS, x = 0.4) 7×10^{-18} (GITT, x = 0.33)	[14]
2	Solid state synthesis	0.5-2 μm	S - not specified A = 2 cm^2	~160 at (C/20)	$10^{-13} – 10^{-14}$ (EIS)	[15]
3	Hydrothermal synthesis	200-400 nm	S = 16 $m^2 \cdot g^{-1}$ (BET) A - not specified	~98,122,125 at (0.5C) ~125,128,136 at (0.2C)	03-2.2 $\times 10^{-14}$ (CV)	[16]
4	Solid state synthesis	400 nm	A = 0.000786 cm^2 S - not specified	~140 at (1C)	2×10^{-10} (CV) 4×10^{-11} (CV)	[17]
5	Solid state synthesis	184 nm 52 nm	Not specified	160; 133 at (0,1C) 149; 123 at (0,2C) 143; 110 at (0,5C) 137; 101 at (1C) 125; 92 at (2C) 97; 44 at (5C)	$1.1 \cdot 10^{-14}$(EIS) $3.2 \cdot 10^{-14}$(EIS)	[18]
6	Solid state synthesis	1 μm	S - not specified A = 100 cm^2 (SEM)	–	$1.3 \times 10^{-16} – 7.6 \times 10^{-11}$ (GITT) $7 \times 10^{-15} – 2.3 \times 10^{-13}$ (PITT)	[7]
7	Solid state synthesis	2.45 μm	S - not specified A = 1.54 cm^2 (SEM)	142 at (0.3C)	8.6×10^{-11} (CV)	[19]
8	Solid state synthesis	100 nm	S - not specified A = 39.9 cm^2	159 at (1C) 141 at (5C) 124 at (15C) 112 at (20C)	2.4-2.8 $\times 10^{-11}$(CV) 2-2.4 $\times 10^{-13}$ (EIS) $10^{-11} – 10^{-14}$ (GITT)	[20]
9	Sol-gel synthesis	50 nm	S = 34.5 $m^2 \cdot g^{-1}$ A - not specified	~160 at (0.1C)	4×10^{-16} (CITT, min at 3.5 V)	[21]
10	Solid state synthesis	–	S - not specified A = 2.23 cm^2 (geom.)	–	$10^{-11} – 10^{-13}$ (PITT) $10^{-11} – 10^{-13}$ (EIS)	[22]

TABLE 1.

In this regard, the works in which a set of electroanalytical methods is presented, are of particular interest. Low-amplitude techniques which do not cause a significant change in the concentration of intercalates should be used among them.

The goal of this study is to determine the diffusion coefficient of lithium in the structure of $LiFePO_4$ from the LiBOB-containing electrolytes using modern methods of CVA and SEI, as well as a comparative analysis of the obtained results.

EXPERIMENTAL

Synthesis of the carbon composite $LiFePO_4$/C has been described in our previous work[23]. The amount of carbon additive in the composite is 2%. The 0.6 molal solution of lithium bis-(oxalato)borate (LiBOB) in an equimolar mixture of ethylene carbonate (EC) (Suprapur, Scharlau Chemie, Spain) and dimethyl carbonate (DMC) (99%, Aldrich) used as electrolyte. Comparative characteristics of the synthesized composite $LiFePO_4$/C has been carried out with a commercial sample of Life Power® P1 (Phostech Lithium, Canada).

The sample for the study of its morphology has been prepared by coating the powder of $LiFePO_4$/C composite on the brass table, followed by the gold layer on the ion sprayer FINE COAT JFC-1100. The sample image was prepared by the scanning elec-

tron microscope JSM-6060 LA (JEOL, Japan) at a voltage of 30 kV.

Cathode mass for electrochemical studies was prepared by mixing the $LiFePO_4$/C composite, carbonized black and polyvinylidene, in the ratio of 0.8: 0.1: 0.1. The resulting mass is applied to a stainless steel substrate (S = 1 cm^2). The electrodes were dried under vacuum at a temperature of 120÷130^{0}C during the5 ÷6 hours. All operations for the preparation of electrolyte and the cell construction were performed in the dry box. Electrochemical measurements of samples were performed using the potentiostate IPC Compact (Russia). The diffusion coefficients of the lithium ions in the $LiFePO_4$ structure were calculated using the data obtaining bythe method of impedance spectroscopy. Electrochemical impedance spectra were recorded on an electrochemical module Autolab-30 PGSTAT302N Metrohm Autolab, equipped by the FRA module (Frequency Response Analyzer) in the range of 3.10 – 106 Hz. Its management was done with Autolab 4.9 at the amplitude of the disturbing signal ±5 mV followed by the Zview 2.0.

RESULTS AND DISCUSSION

The data on the surface morphology of the composite LiFePO4/C under the SEM image are shown in Figure 1. As is evident, at an annealing temperature equal to 650°C particle aggregation occurs due to sintering. The heterogeneity of particle size, according to the image is 0.1÷1.0 mm. This difference

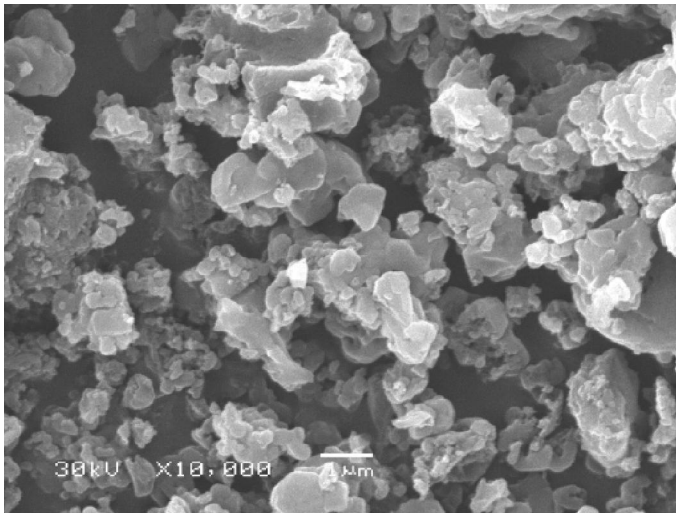

Figure 1 : SEM image of $LiFePO_4$/C

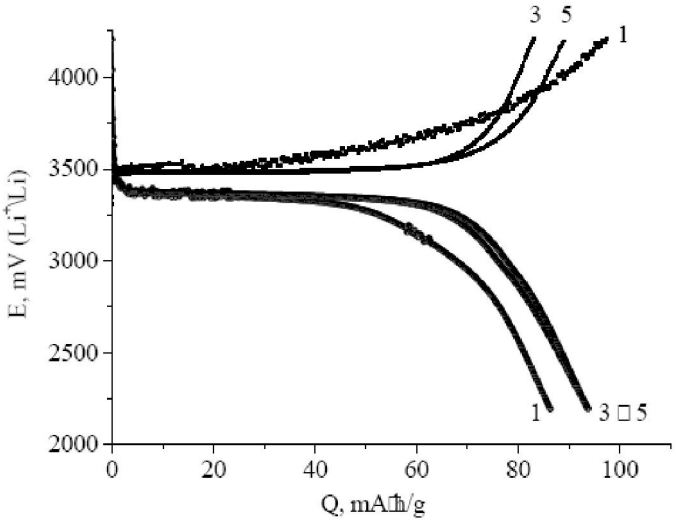

Figure 2 : The charge/discharge curves of the $LiFePO_4$/C electrode, i = 45 mA/g. 1, 3, 5 – cycle numbers

in particle size can provide for implementation of high current restriction during the work of lithium-ion battery[24].

Cycling of electrode from the LiFePO4/C composite was carried out in the potential range of 2.2÷4.2 V, rel. Li^+/Li (Figure 2). The plato is observed in the charge-discharge curve in the potential range of 3.4÷3.5 V (rel. Li^+/Li). It is responsible for the intercalation/deintercalation of lithium in the structure of olivine. The low specific capacity in the 1st cycle is associated with forming of the conductive solid electrolyte membrane (SEI) on the electrodes.

When cycling $LiFePO_4$/C composite for 100 cycles (Figure 3), an increase of specific capacity of the material is observed. It indicates its gradual elaboration during the intercalation/deintercalation of lithium. The gap between the 40th and 80th cycles is related to providing of the diffusion research by the CV and EIS methods).

By increasing the discharge current density from 0.1 C to 10 C there is a decrease in specific capacity of the sample from 110 to 40 mA·h/g (Figure 4). Change of the specific capacity by increasing the discharge current density for samples of $LiFePO_4$/C and Life Power® P1 is in a good agreement with a density of 0.5 S.

Cyclic voltammograms of the $LiFePO_4$/C electrode are shown at the Figure 5 and display the process of intercalation/deintercalation of lithium ions

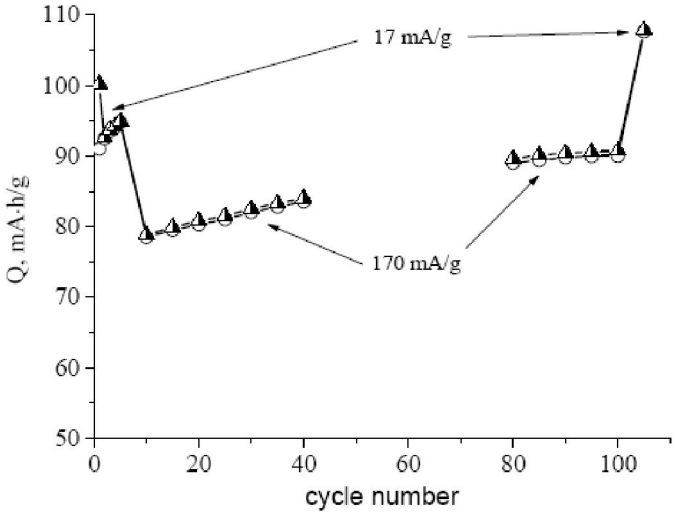

Figure 3 : Change of the specific capacity during the cycling electrodewith $LiFePO_4$/C composite

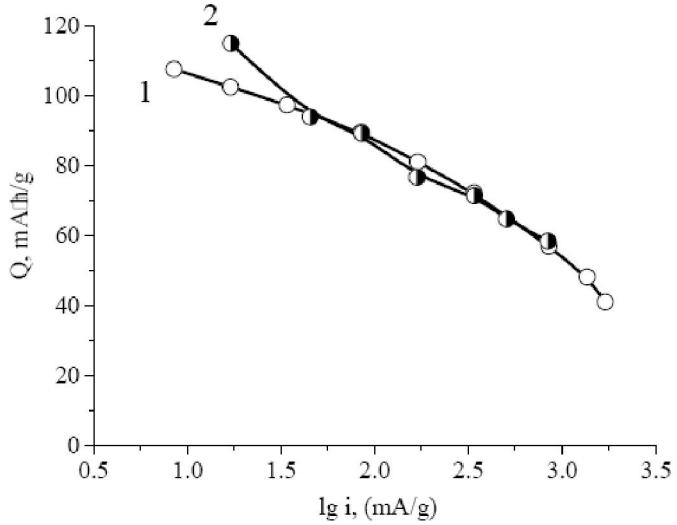

Figure 4 : Change of the specific capacity of $LiFePO_4$/C electrode depending on the density of discharge current: 1 – synthesized sample; 2 – commercial sample Life Power® P1

in the olivine structure, after the formation of passive membranes on electrodes. With increasing of the potential scan rate, there is a shift of anodic peak towards higher potential values and cathodic peak – to lower values.

This fact indicates an increase in the irreversibility of the reaction of lithium intercalation/ deintercalation. It should be noted that the shift of the peak positions on the scale of the potential with increasing scan rate is observed even for ultra-thin electrodes with minimum speeds of potential sweep, indicating a change in the initial composition of the electrode, and gives the calculated values of the effective parameters.

The calculation of the diffusion coefficient of lithium ion in the olivine structure has been carried by the Rendls–Shevchik equation[25], which is as follows at the 25°C:

$$I_p = 2{,}69 \cdot 10^5 n^{\frac{3}{2}} A D_{Li}^{\frac{1}{2}} \vartheta^{\frac{1}{2}} C \qquad \textbf{(1)},$$

wherein

n – number of electrons participating in the elementary act; A – area of the electrode, cm^2; D_{Li} – lithium diffusion coefficient, cm^2/s; ϑ – rate of potential sweep, V/s; c– the initial concentration of vacancies in the intercalates (cathodic process) or the initial concentration of lithium (for anodic process), mol/L.

It should be noted that most of the authors in the equation (1) using the value of the geometric area of electrode, which leads to high results of the value of diffusion coefficient for lithium ions (see TABLE 1). At the same time, the determination of the surface area according to the classical BET method (Bernauer-Emmett-Teller) may introduce errors in its value due to the presence of carbon significant surface in the LiFePO4/C composite[26], which ultimately results in for low values of the diffusion coefficient of lithium. In this study, to determine the surface area of the composite electrode the mean particle radius from the SEM image (an average particle diameter of 500 nm), has been used. The formula for calculating the surface area[24, 27, 28], is as follows:

$$A = \frac{3}{r \cdot \rho} \qquad \textbf{(2)},$$

wherein

r – the radius of the particle, cm; ρ – density of the $LiFePO_4$ (ρ = 3,6 g/cm^3).

Figure 6 shows the values of the anodic and cathodic current peaks in coordinates I_p – f($\sqrt{\vartheta}$), appropriate to the linearization of equation (1). Presented results confirm the assumption about the diffusion nature of the limiting stage. Linearization standard error was (R^2 = 0.996 – 0.999). Calculated according to equation (1), the magnitude of the averaged diffusion coefficient for lithium ions is $2.06 \cdot 10^{-14}$ and $1.07 \cdot 10^{-14}$ cm^2/s for the anodic and cathodic processes, respectively.

The impedance spectra obtained with varying degrees of lithium intercalation into the structure of

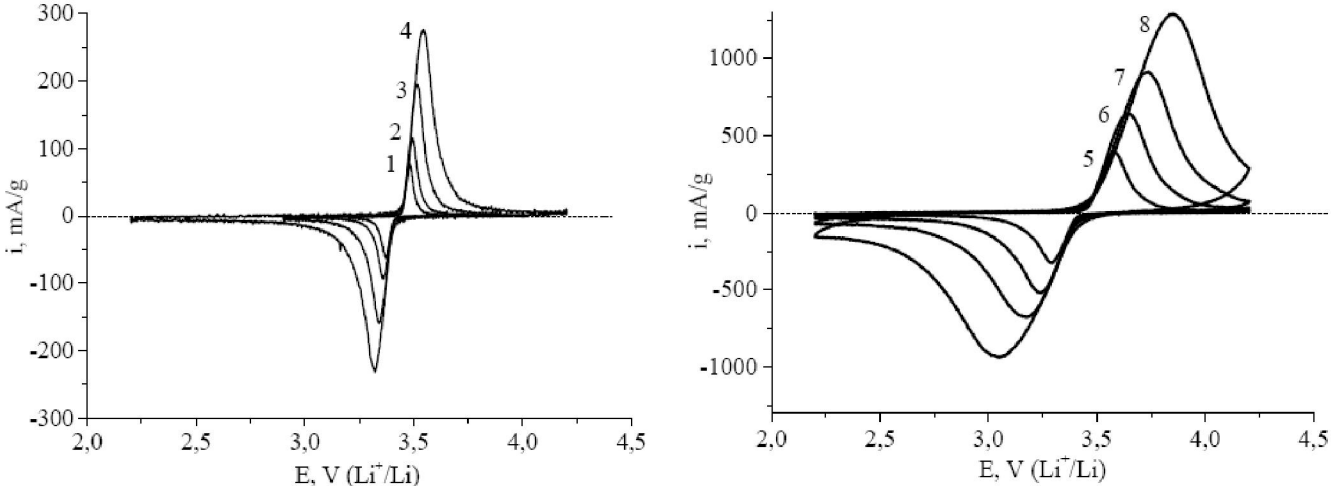

Figure 5 : Cyclic voltammograms sample $LiFePO_4$/C at different rates of the potential sweep: 1 – 0.01 mV/s; 2 – 0.02 mV/s; 3 – 0.05 mV/s; 4 – 0.1 mV/s; 5 – 0.2 mV/s; 6 – 0.5 mV/s; 7 – 1 mV/s; 8 – 2 mV/s

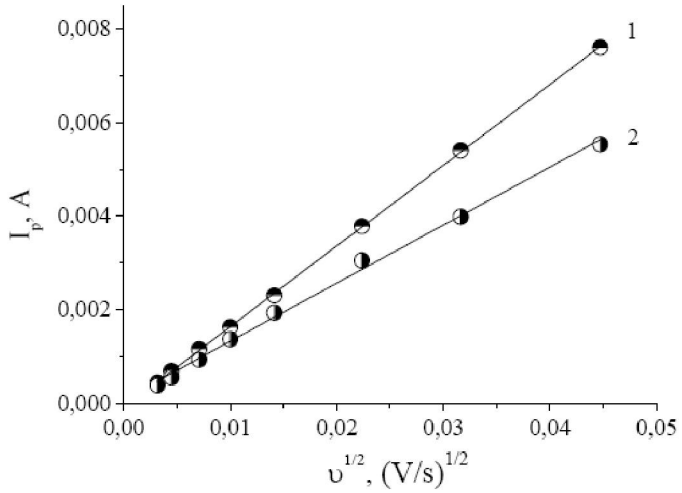

Figure 6 : The dependence of the current of anode (1) and cathode (2) peaks from the rate of potential sweep

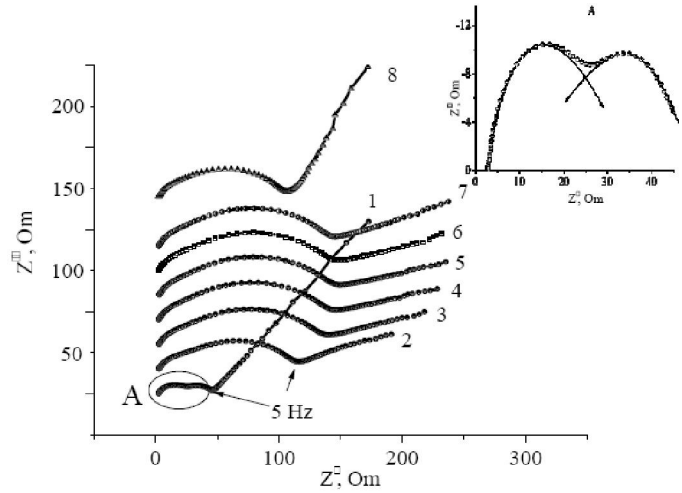

Figure 7 : Nyquist diagram for various degrees of lithium intercalation (x) into the structure of Li_xFePO_4 in value x: 0.862(1), 0.786(2), 0.710(3), 0.634(4), 0.558(5), 0.482(6), 0.406(7), 0.330(8); A – insert, figure Z2 , Z3 at f=5 Hz

Li_xFePO4 are presented at the Figure 7. In all cases, the impedance spectra represent the center of the semicircle below the x-axis - in the high and mid-range, and a linear portion extending at different angles – in the low-frequency region. In this case, the impedance spectrum attended two arcs (Figure 7A) which are effective feedbacks of the boundary migration processes SEI/solution, conjugated in the bulk transport SEI, and transfers across the boundary SEI/intercalates flowing together with the diffusion layer in the intercalation.

The obtained spectra are satisfactorily modeled by electrical equivalent scheme (EPS), are presented at the Figure 8.

Here, instead of the classical capacity we used the CPE element (constant phase element). Its physical meaning is not fully determined, but some authors consider it because of diffusion to non-fairness surface[29-30], or the accumulation of charge directly on the surface. It should be noted that the choice of the EPS to simulate the impedance spectra is an important consideration in interpreting the results since the same spectra can be satisfactorily interpreted via various schemes, so-called principle of identical equivalent circuits consisting of identical elements and differing by the scheme of its compounds, but adequately describe the mechanism of electrode reactions. In this case, we need more independent information on the prediction mechanism of electrode process. We used the experiment of cyclic voltammetry for this purpose.

The physical picture of processes, occurring in

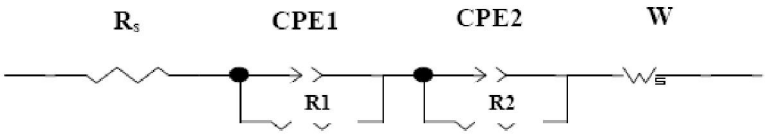

Figure 8 : Electrical equivalent scheme used for the simulation of impedance spectra of the intercalation electrode

TABLE 2 : Informative parameters of electrode material based on Li_xFePO4 calculated using EPS, according to the impedance spectroscopy data

x in Li_xFePO_4	R_s, Ohm		R2, Ohm		R3, Ohm		CPE1, Ohm		CPE2, Ohm		W, Ohm	
	Mean	Err. %	Mean	Err. %	Mean	Err. %	Mean	Err. %	Mean	Err. %	Mean	Err. %
0.330	2.642	0.58	16.58	4.71	21.97	1.58	0.91	2.85	0.88	0.45	14.84	180.8
0.406	2.642	1.58	72.94	2.44	27.38	5.76	0.87	1.56	0.82	1.05	156.9	149.8
0.482	2.576	2.23	104.6	2.37	18.88	11.25	0.81	1.55	0.87	1.91	152.8	181.6
0.558	2.362	2.82	116.1	3.05	14.53	19.1	0.79	2.03	0.91	3.22	237	39.93
0.634	2.774	2.29	119.3	2.57	13.72	16.96	0.795	1.74	0.93	2.98	16.9	8.64
0.710	2.370	2.44	118.2	2.82	14.06	18.16	0.796	1.85	0.93	3.06	6.33	6.67
0.786	2.465	1.94	111.6	2.57	17.51	13.61	0.82	1.59	0.90	2.07	5.62	7.35
0.862	2.818	0.97	71.44	8.54	24.49	22.49	0.86	3.44	0.82	1.68	11.17	12.70

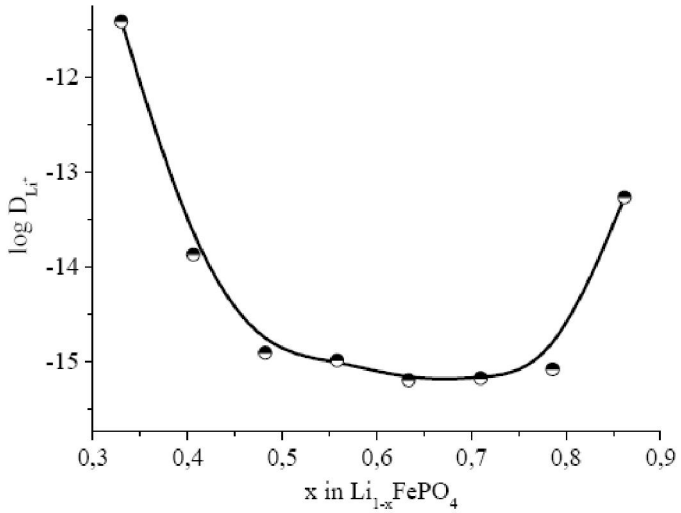

Figure 9 : Change of the diffusion coefficient of lithium ion in the olivine structure depending on the degree of intercalation

the system, is mainly clear thanks to numerous studies. Transport of the lithium ions sequentially passes through the electrolyte solution in the pores of the separator, solid electrolyte layer, and the interphaseboundary. Relevant stages of this process are reflected in the EPS, and their numerical values as resistance of the electrolyte in the pores of separator (R_s) and the transfer resistance of lithium ion through the SEI/intercalates boundary (Rct), Warburg impedance W responsible for lithium diffusion were calculated using this scheme and presented in TABLE 2.

The equation for the diffusion coefficient of lithium when changing its degree of intercalation into the Li_xFePO_4 [7, 31] is as follows:

$$D_{Li} = \frac{1}{2}\left[\left(\frac{V_m}{F \cdot A \cdot \sigma}\right)\left(\frac{dE}{dx}\right)\right]^2 \quad \textbf{(3)},$$

wherein

V_m – molar volume, mol/cm^3, F – Faraday constant, σ – Warburg factor, Ohm·s$^{1/2}$ {determined from the linear dependence of the Z2 or Z3 – f ($\omega^{1/2}$)}, $\frac{dE}{dx}$ – changes in electrode potential at various

degrees of lithium intercalation (x).

The change of the diffusion coefficient of lithium ion in the structure of $Li_{1-x}FePO_4$ is shown at the Figure 9. The resulting dependence is characterized by a minimum of a wide range of changes in the degree of intercalation (x), which is in a good agreement with the results obtained by other authors[32, 33].

The course of the obtained dependence is due to the interfacial interactions between the lithium ions and oxygen atoms in the structure of $LiFePO_4$[6]. Peixin et al.[34] noted that the diffusion rate of lithium ions is mainly dependent on the structural characteristics of the crystal. The rate of diffusion is higher when the distance between the oxygen atoms in the $LiFePO_4$ and the lithium ion is greater.

The D_{Li} values obtained by the CVA and SEI methods are in good agreement with published data (see TABLE 1). It indicates the correctness and the reliability of obtained results.

CONCLUSIONS

Medium temperature (650°C) synthesis of the $LiFePO_4$/C composite with olivine structure allows to obtain powders with a particle size 0,1÷10 microns. The charge-discharge curves of the electrode from these powders have a horizontal portion at a potential of 3.4 and 3.5V, corresponding to the intercalation/deintercalation of lithium in the structure of olivine. Dependency analysis of anode (cathode) peaksof $I_p$point from the potential sweep velocity v indicates the diffusion nature of the lithiating step of electrode process. This conclusion is also supported by the dominant influence of the Warburg impedance in the structure of the electrode impedance (our data) and a view of the dependence of w from x in Li_xFePO_4/C (a curve with a broad minimum in the x = 0.406–0.558, see TABLE 2). We find (Figure 9) the similar graph in the same x area (log D_{Li-x}). It should also be noted that the specific discharge capacity of the synthesized $LiFePO_4$/C sample and commercial (Life Power) are the same at the discharge currents greater than 0.5 C.

REFERENCES

[1] A.K.Padhi, K.S.Nanjundaswamy, S.Masquelier; J.Electrochem.Soc., **144**, 1609 **(1997)**.

[2] N.A.Burmistrova, V.O.Sycheva, A.V.Churikov; Electrochem.Energy, **9(4)**, 188 **(2009)**.

[3] W-J.Zhang; J.Power Soc., **196**, 2962 **(2011)**.

[4] A.K.Padhi, K.S.Nanjundaswamy, J.B.Goodenough; Electrochem.Soc.Meet.Abstr., **96(1)**, 73 **(1996)**

[5] A.K.Padhi, K.S.Nanjundaswamy, J.B.Goodenough; J.Electrochem.Soc., **144**, 1188 **(1997)**.

[6] N.V.Korovin, Electrochemistry, **35(6)**, 738 **(1999)**.

[7] A.V.Churikov, A.V.Ivanischev, I.A.Ivanischeva, V.O.Sycheva, N.R.Khasanova, E.V.Antipov; Electrochim.Acta, **55**, 2939 **(2010)**.

[8] W.Weppner, R.A.Huggins; J.Electrochem.Soc., **124(10)**, 1569 **(1977)**.

[9] A.V.Churikov; Electrochem.Energy, **3(3)**, 124 **(2003)**.

[10] A.V.Ivanischev, A.V.Churikov, I.A.Ivanischeva; Electrochemistry, **44(5)**, 553 **(2008)**.

[11] F.Gao, Z.Tang; Electrochem.Acta, **53**, 5071 **(2008)**.

[12] M.D.Levi, G.Salitra, B.Markovsky; J.Electrochem.Soc., **146**, 1279 **(1999)**.

[13] D.Zhao, Y.L.Feng, Y.G.Wang; Electrochem.Acta, **88**, 632 **(2013)**.

[14] P.Prosini, M.Lisi, D.Zane, M.Pasquali; Solid State Ionics, **148**, 45 **(2002)**.

[15] S.Franger, F.Cras, C.Bourbon, H.Rouault; Electrochemistry Solid State, **5**, A231 **(2002)**.

[16] D.Y.W.Yu, C.Fietzek, W.Weydanz, K.Donoue, T.Inoue, H.Kurokawa, S.Fujitani; J.Electrochem.Soc., **154**, A253 **(2007)**.

[17] P.He, X.Zhang, Y.G.Wang, L.Cheng, Y.Y.Xia; J.Electrochem.Soc, **155**, A144 **(2008)**.

[18] G.Huanga, W.Lia, H.Suna, J.Wangb, J.Zhanga, H.Jianga, F.Zhaia; Electrochim.Acta, **97**, 92 **(2013)**.

[19] X.H.Rui, Y.Jin, X.Y.Feng, L.C.Zhang, C.H.Chen; J.Power Soc., **196**, 2109 **(2011)**.

[20] W.L.Liu, J.P.Tu, Y.Q.Qiao, J.P.Zhou, S.J.Shi, X.L.Wang, C.D.Gu; J.Power Soc, **196**, 7728 **(2011)**.

[21] J.Ma, B.Li, H.Du, C.Xu, F.Kang; J.Electrochem.Soc., **158**, A26 **(2011)**.

[22] H.Manjunatha, T.V.Venkatesha, G.S.Suresh; Electrochim.Acta, **58**, 247 **(2011)**.

[23] A.V.Potapenko, E.V.Panov, V.A.Diamant; Ukr.Chim.Zhurn., **7**, 52 **(2014)**.

[24] A.V.Potapenko, S.A.Kirillov; J.Energy Chemistry, **23**, 543 **(2014)**.

[25] G.Gallus; Theoretical foundations of electrochemical analysis, Moscow, 552, **(1974)**.

[26] M.Vujkovič, I.Stojkovič, N.Cvjetičanina, S.Mentus; Electrochim.Acta, **92**, 248 **(2013)**.

[27] K.Wang, R.Cai, T.Yuan, X.Yu, R.Ran, Z.Shao; Electrochim.Acta, **54**, 2861 **(2009)**.
[28] C.Mi, X.Li, H.Zhang; J.Electroanal.Chem., **602**, 245 **(2007)**.
[29] P.Liu, H.Wu; Solid State Ionics, **92**, 91 **(1996)**.
[30] L.Nyikos, T.Pajkossy; Electrochim.Acta, **31**, 1347 **(1986)**.
[31] C.Ho, I.D.Raistrick, R.A.Huggins; J.Electrochem.Soc., **127**, 343 **(1980)**.
[32] T.Xin-Cun, L.Lian-Xing, L.Qiong-Lin; Electrochim.Acta, **54**, 2389 **(2009)**.
[33] K.Tang, X.Yu, J.Sun; Electrochim.Acta, **56**, 4869 **(2011)**.
[34] Z.Peixin, Z.Dongyun, Y.Qiuhua; Solid State Sciences, **13**, 1510 **(2011)**.